Journal of Applied Polymer Science

Recycling of Reactive Dye Using Semi-Interpenetrating Polymer Network from Sodium Alginate and Isopropyl Acrylamide

V. Dhanapal,[1] K. Subramanian[2]

[1]Department of Physical Sciences, Bannari Amman Institute of Technology, Sathyamangalam 638401 Erode Dt, Tamil Nadu, India
[2]Department of Biotechnology, Bannari Amman Institute of Technology, Sathyamangalam 638401 Erode Dt, Tamil Nadu, India
Correspondence to: K. Subramanian (E-mail: drksubramanian@rediffmail.com)

ABSTRACT: A sequence of semi-interpenetrating polymer network (semi-IPN) were synthesized by free radical photo copolymerizing acrylic acid and isopropyl acrylamide (NIPAAm) in aqueous sodium alginate (NaAlg). Their structures (FT-IR), thermal stability (TG/DTG), morphology (SEM), mechanical properties, reactive blue 4 (RB 4) dye adsorption (624 mg/g) and its dying characteristics, reusability of dye and adsorbent were evaluated. TG thermograms of semi-IPN in air revealed zero order kinetics for initial step thermal degradation with an activation energy of 68.68 kJ/mol. Dye adsorption showed best fit for Langmuir adsorption isotherm and the kinetics followed pseudo-second-order model. The water and dye diffusion kinetics followed non-Fickian mechanism. The changes in thermodynamic parameters namely Gibbs free energy (ΔG°), entropy (ΔS°) and enthalpy (ΔH°) indicated that the adsorption was spontaneous and exothermic process for RB 4/semi-IPN system. © 2014 Wiley Periodicals, Inc. J. Appl. Polym. Sci. **2014**, *131*, 40968.

KEYWORDS: activation energy; adsorption kinetics; dye recycling; FT-IR; thermodynamics; thermogravimetry

Received 10 February 2014; accepted 4 May 2014
DOI: 10.1002/app.40968

INTRODUCTION

The increased population and industrialization caused water and soil pollution by the discharged effluents from garbage and industries such as dying, paper, plastic, leather, food, mineral processing[1] and so forth. without proper treatment leading to various health hazards both to mankind and other living beings. Among them textile dye effluents contributes a lot by discharging huge quantity of unabsorbed residual dyes which are having low biochemical oxygen demand and high chemical oxygen demand[2] values. Many synthetic organic dyes from effluent are highly toxic and endanger the aquatic life[3] and the environment.[3] The presence of such reactive dyes in water bodies may be mutagenic and carcinogenic[4] and can cause severe damage to the liver, digestive and the central nervous system[2] of human beings and affect agricultural cultivation[2] and underground water quality.[2] Hence, it is necessity to remove colored material from the effluent before being discharged into land and water using any one of the following physico-chemical or biological methods. Among them the adsorption technology which employs activated carbon,[2] natural clays,[5] modified clays,[6] fly ash,[7] and so forth. as adsorbents is generally considered to be a cost effective method to bring down the concentration of unabsorbed dyes in dye effluent.[8] In recent years IPN and semi-interpenetrating polymer network (semi-IPN) are progressively being used to remove the colors, toxic substances, heavy metals and other pollutants from effluent[9,10] through adsorption mechanism.[11] They comprise minimum of two polymers exhibiting different characteristics and it is prepared by generating a polymer in the presence of another preformed linear polymer.[9–11] IPN and semi-IPN can produce synergistic effect by sharing the properties of both the polymers consequently avoiding the limitations of natural as well as synthetic polymers.[12] They exhibit high equilibrium swelling (ES) in water or aqueous solutions when the preformed macromolecules used to have high hydrophilicity and flexibility. The high hydrophilicity may be achieved by choosing the pre polymer with polyelectrolytic nature or by choosing a linear polymer having the functional groups such as carboxylic acid, amine, hydroxyl, amide, and sulfonic acid groups in the polymer chain.[13] Because of these properties, they are finding widespread applications[14,15] in bioengineering, biomedicine, agriculture, food industry, water purification, separation process, effluent treatment, and so forth.

In the present investigation, NaAlg was used as preformed macromolecule for synthesizing semi-IPN. The primary choice of NaAlg is due to the attractive combination of availability, price, and its performance[16] in effluent treatment. NaAlg, a natural ionic hydrophilic linear polysaccharide containing β-D-mannuronic acid and α-L-guluronic acid (Scheme 1) with —OH and —COO^- groups are commonly used in the synthesis of hydrogels for different applications with improved mechanical

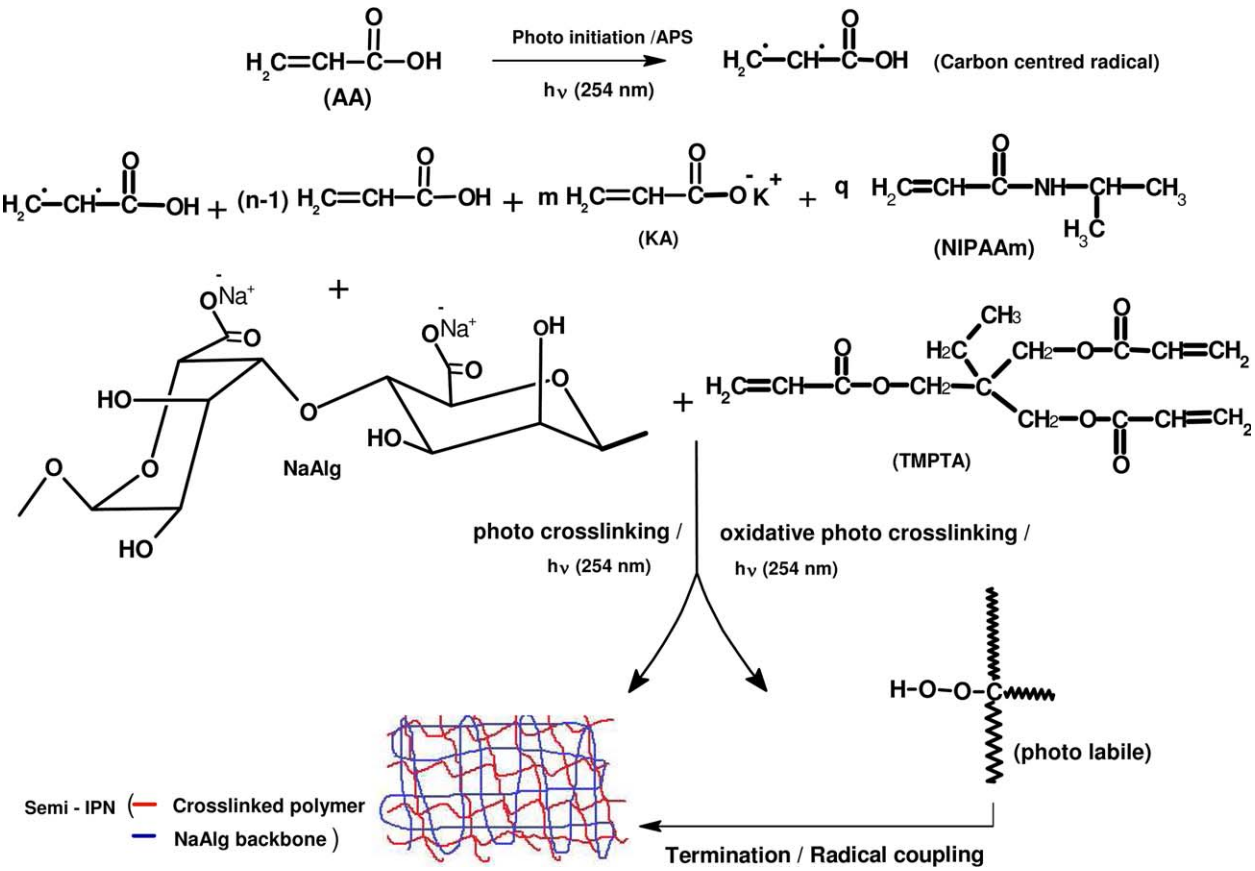

Scheme 1. Photo synthesis mechanism for formation of semi-IPN. [Color figure can be viewed in the online issue, which is available at wileyonlinelibrary.com.]

properties.[14] The sugar residues in NaAlg can either be arranged in blocks or they can be randomly distributed.[17] Moreover, NaAlg-based semi-IPN was shown to be an excellent adsorbent for the removal of colored materials and toxic heavy metal ions from industrial effluent.[16–19] Hence, semi-IPN is viewed as one of the potential adsorbent for recycling of colored materials.[11,18] The present investigation involves the synthesis and evaluation of potential adsorbent to recycle reactive dye from the textile dye effluent.

EXPERIMENTAL

Materials

Acrylic acid (AA) (Himedia, Mumbai), ammonium persulphate (APS) (NICE, Cochin) was used after purification by vacuum distillation (700 mmHg) and recrystallization with double distilled water respectively. Potassium hydroxide (KOH), NaAlg, trimethylolpropane triacrylate (TMPTA) (Himedia Mumbai), NIPAAm (Aldrich), acetone, methanol, isopropanol (Rankem, New Delhi), sodium chloride (NaCl), sodium carbonate (Na_2CO_3) (Merck), reactive blue 4 (RB 4) (Sigma-Aldrich, molecular weight = 637.43, color index no = 6,1205, λ_{max} = 595 nm) were used as received, and the chemical structure of RB 4 is shown in Figure 1(a).

Photo Synthesis of Semi-IPN

For the photo synthesis of semi-IPN using AA, KA (potassium acrylate), NIPAAm with TMPTA were taken in a quartz tube containing NaAlg aqueous solution (0.25–1.5 g, Table I) using APS (0, 3, 6, 9, and 12 $\times$ 10^{-3} *M*) initiator with the polymerization volume of 40 mL. The solution was nitrogen purged for 20 min to remove the dissolved oxygen. Then, the homogenous mixture was irradiated with UV light (254 nm) for the durations of 0, 2, 4, 6, 8, and 10 h by keeping the distance between the lamp and solution surface in the tube as 15 cm. During irradiation, monomers and crosslinker was photo polymerized in the presence of preformed macromolecules.[11,13] After the polymerization, the obtained semi-IPN was recovered by repeatedly washing with ice cold methanol immediately to remove unreacted monomers. The semi-IPN thus obtained were cut into small pieces and dried to constant weight at 50°C under vacuum. The dry polymer was powdered and further purified by Soxhlet extraction using acetone–methanol (1 : 1, v/v) at 50°C for 3–4 days, powdered, sieved (mesh size 100 and 150 μm) and stored after vacuum drying.

Chemical Characterization of Photo Synthesized Semi-IPN

FT-IR spectra of NaAlg, semi-IPN, virgin and recovered RB 4 were recorded in KBr pellet for the spectral range 400–4000 cm^{-1} using Shimadzu FT-IR–8400S by accumulating 48 scans at a resolution of 2 cm^{-1}. Thermal degradation studies were performed on TGA Q 500 V20.10 Build 36 with a sample size of 1–3 mg under air at a heating rate of 10°C min^{-1} for the temperatures ranging from ambient to 800°C. The concentration of RB 4 in the synthetic dye effluent was spectrophotometrically estimated by measuring the absorbance at 573 nm using

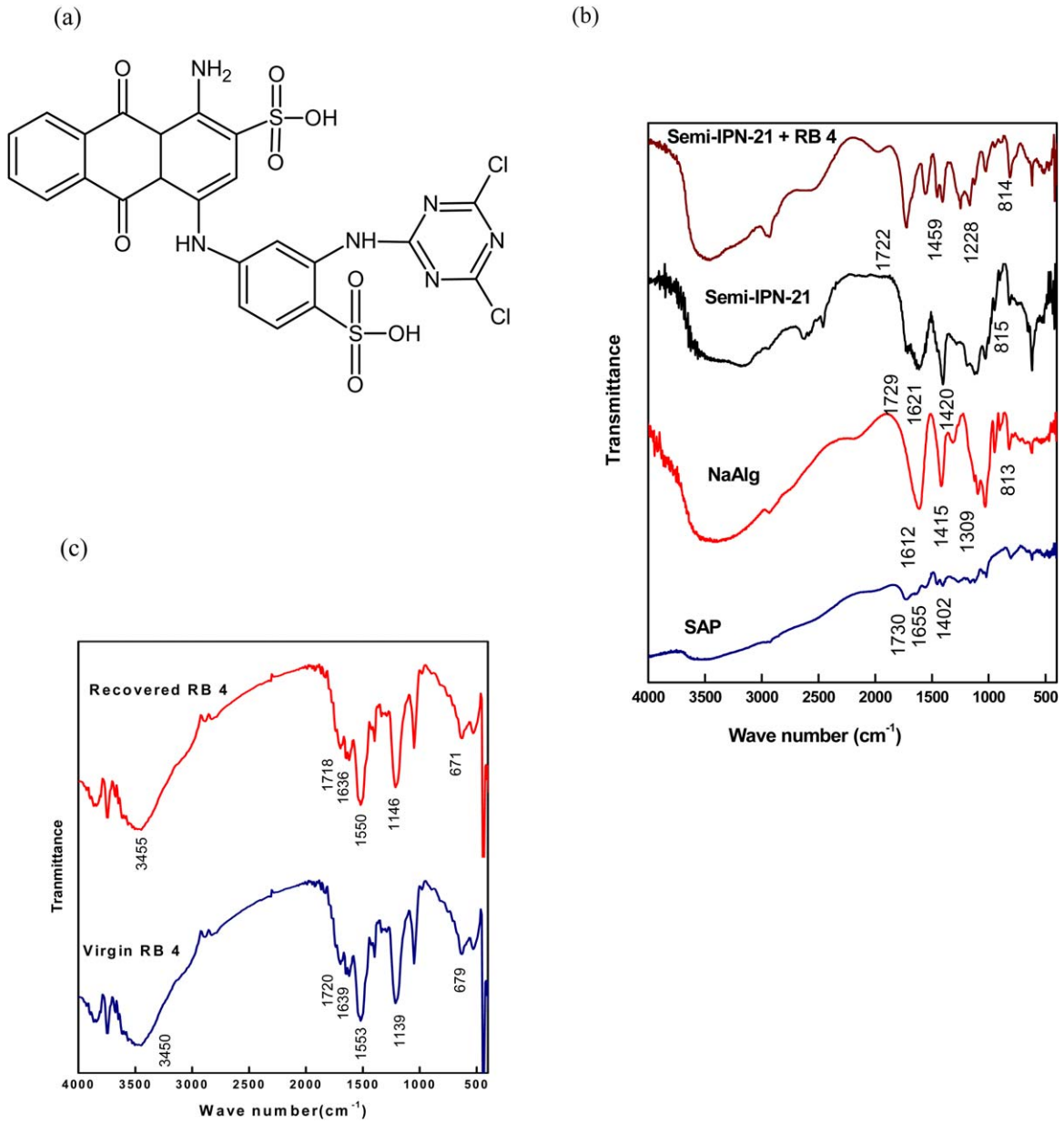

Figure 1. Chemical structure of RB 4 (a), FT-IR spectra of SAP (b), NaAlg (b), Semi-IPN 21 (b), Semi-IPN 25 (b), virgin (c) and recovered (c) RB 4 dye. [Color figure can be viewed in the online issue, which is available at wileyonlinelibrary.com.]

UV–visible absorption spectrometer (Perkin Elmer Lambda 35). The virgin and recovered RB 4 dye concentration in the dyed cotton fabrics was spectrophotometrically estimated by measuring the absorbance at 602 nm using Gretag Macbeth spectrophotometer. SEM (Scanning electron microscopy) micrographs of semi-IPN, SAP and RB 4 adsorbed semi-IPN 21 at different magnifications were recorded using ZEISS EVO Series SEM model EVO 50. The equilibrium swelled and lyophilized semi-IPN, SAP and powdered SAP samples were used for recording SEM micrographs.

Swelling Measurement

The degree of swelling of semi-IPN was measured using a tea bag as discussed elsewhere[20] in double distilled water by taking 0.1 g of sieved sample in 200 mL of distilled water at 30°C under ES conditions (4 h). The swelling profiles were constructed by plotting the water-absorbed during various time intervals at 30°C against time. The ES was calculated by taking an average of three absorption measurements using the eq. (1)

$$\mathrm{ES} = \frac{W_s - W_d}{W_d} \quad (1)$$

where W_s and W_d are the weights of the swollen gel and the dry sample respectively.

Measurement of Mechanical Properties

The mechanical properties of the water swollen semi-IPN 21 and SAP were measured at room temperature in terms of elastic modules and ultimate tensile strain using tensile-compressive

Table I. Composition of Semi-IPN Samples and Their Equilibrium Dye and Water Uptake Capacity

IPN sample code	*S/A* Mole ratio[a]	NIPAAm (M)	TMPTA (M)	Weight of NaAlg (g)	Dye adsorption in column mode (mg g^{-1})	Water uptake (g g^{-1})
semi-IPN 1	0	0.05	0.05	0.5	228.56	319.77
semi-IPN 2	0.0316	0.05	0.05	0.5	236.61	325.72
semi-IPN 3	0.0562	0.05	0.05	0.5	270.45	342.26
semi-IPN 4	0.5723	0.05	0.05	0.5	295.34	378.26
semi-IPN 5	6.3095	0.05	0.05	0.5	258.43	290.38
semi-IPN 6	28.1838	0.05	0.05	0.5	211.33	281.67
semi-IPN 7	446.684	0.05	0.05	0.5	191.12	279.77
semi-IPN 8	0.5723	0.05	0.0025	0.5	320.45	798.98
semi-IPN 9	0.5723	0.05	0.005	0.5	395.56	843.78
semi-IPN 10	0.5723	0.05	0.0375	0.5	356.76	675.98
semi-IPN 11	0.5723	0.05	0.0625	0.5	345.24	503.45
semi-IPN 12	0.5723	0.05	0.075	0.5	328.15	489.76
semi-IPN 13	0.5723	0.05	0.0875	0.5	301.91	508.67
semi-IPN 14	0.5723	0.0125	0.005	0.5	456.87	678.46
semi-IPN 15	0.5723	0.025	0.005	0.5	461.34	728.34
semi-IPN 16	0.5723	0.0375	0.005	0.5	472.87	783.81
semi-IPN 17	0.5723	0.0625	0.005	0.5	485.78	968.54
semi-IPN 18	0.5723	0.075	0.005	0.5	480.62	756.52
semi-IPN 19	0.5723	0.0875	0.005	0.5	473.76	412.97
semi-IPN 20	0.5723	0.0625	0.005	0.25	530.97	1012.47
semi-IPN 21	0.5723	0.0625	0.005	0.75	624.05	993.26
semi-IPN 22	0.5723	0.0625	0.005	1	577.73	734.98
semi-IPN 23	0.5723	0.0625	0.005	1.25	521.56	645.23
semi-IPN 24	0.5723	0.0625	0.005	1.5	510.97	623.42
semi-IPN 25[b]	0.5723	0.0625	0.005	0.75	391.42	467.56
SAP	0.5723	0.0625	0.005	0	387.43	1130.21

[a] *S/A* ratio: (Potassium acrylate/AA) constant amounts of AA (1.27 *M*) and APS(0.009 *M*) were taken in all the experiments for a polymerization volume of 40 mL.
[b] Photo polymerized without APS.

tester (Tensilon RTC-1310A, Orientec Co.).[19,21] Figure 2 has showed the physical appearance of semi-IPN 21 under compression. The compressive test of semi-IPN and SAP were performed using cylindrical gel samples of 10-mm diameter and 5-mm thickness and these samples were set on the lower plate separately and compressed by the upper plate, which was connected to a known loaded cell with a strain rate of 10% min^{-1} till the onset of damage. The corresponding ultimate compressive strain and moduli values were also measured for semi-IPN 21 and SAP. The strain under compression is defined as the change in the thickness relative to the thickness of the specimen. For the tensile tests of semi-IPN 21 and SAP, samples were cut into dumbbell shapes and stretched parallel to the sample axis using a clamp attachment at a strain rate of 10% min^{-1}. Strain rates were referenced to the initial thickness of length of specimen. Failure points of compressive and tensile tests were determined from the peak of the stress–strain curve.

Dying Using Virgin and Recovered RB 4

The dyebath (2%) for dying process was prepared using cold brand RB 4 dye and keeping material: liquor ratio as 1 : 20. Then, 5 g of well scoured, bleached, and wetted cotton fabric was dipped in the dyebath for 10 min. The dye exhausting agent (NaCl, 3.5 g) was added in two installments and the dyebath was set aside for another 20 min, and subsequently 20 mL dye fixing agent (Na_2CO_3, 0.45 g) was added[22,23] to the dyebath and allowed for dye fixation for another 60 min. The cold and hot water rinsing followed by detergent washing removed the unfixed dye from the fabric[21,22] and these fabric washings with water were added into the dye bath solution. The visible absorbance for dyed and air dried fabric were recorded. The unfixed dye in dyebath after dying was recovered by passing through semi-IPN 21 in a column followed by elution using isopropanol eluent, and the dye was recovered through by distilling out of isopropanol. The adsorption–desorption of RB 4 was performed over five times for the same adsorbent to determine the frequency of reusability of semi-IPN 21 in effluent treatment. After each cycles of adsorption–desorption, semi-IPN 21 was washed with distilled water thrice and then dried in an air oven at 60°C for reuse. The amount of total residue along with RB 4 in the solution was quantified after evaporation. Then, the recovered residue was dissolved in 100 mL double

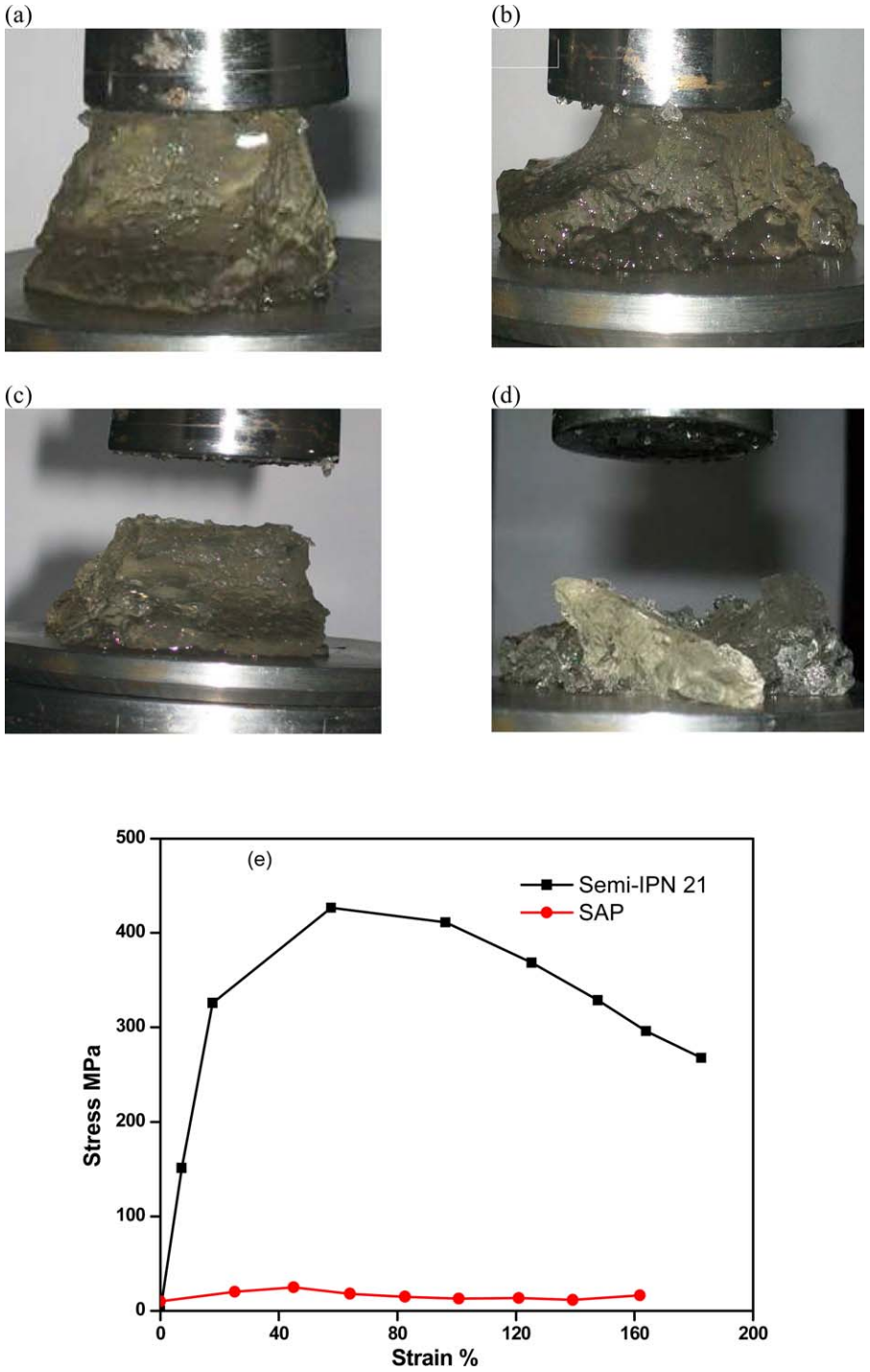

Figure 2. Photographs of semi-IPN 21 with 90% water content before compression (a), during compression (b), after compression (c), SAP after compression (d) and stress–strain curve for semi-IPN 21 and SAP (e). [Color figure can be viewed in the online issue, which is available at wileyonlinelibrary.com.]

distilled water and the concentration of RB 4 in the residue was determined spectrophotometrically after appropriate dilution. Another dye bath was prepared with same dyebath concentration using recovered RB 4 for dying and the solid state absorption spectra were recorded for comparing the absorption spectra. The color fastness properties of the dyed fabric with virgin and recovered RB 4 were also determined (under sunlight and 0.2% soap solution containing 0.5% Na_2CO_3 solution) over a period of 12 h by recording and comparing the absorption spectra.

Adsorption Studies

Batch Mode. The stock solution of RB 4 (7.84×10^{-3} *M* (= 4.9 g) was prepared using distilled water, and a series of

concentrations of (1, 2, 3, 4, and 5 × 10^3 mg L^{-1}) dye solutions were prepared by appropriate dilution of stock solution in the presence NaCl (5 g L^{-1}) as dye exhausting agent and Na_2CO_3 (1.5 g L^{-1}) as dye fixing agent.[21–23] The adsorption study of RB 4 was investigated as a function of the structure of adsorbent and environmental factors like time, temperature, pH, and ionic strength of the medium. All batch mode adsorption experiments were carried out by mixing 0.1 g of semi-IPN 21 with 100 mL of aqueous solution (RB 4) taken in a 250 mL conical flask. The flasks were shaken in a thermostatic mechanical shaker for 24 h to provide sufficient contact time for equilibrium to be established between the solid and liquid phases at 30°C and 120 rpm. The experiments were conducted in triplicate and average values are reported. The solution was separated from the adsorbents using a 100-mesh (nylon) sieve and the concentration of RB 4 in dye effluent before and after the adsorption was measured spectrophotometrically after suitable dilutions. The equilibrium adsorption of RB 4 was calculated (Table I) using the mass balance eq. (2)

$$q_e = (C_i - C_e)\frac{V}{W}\ \text{mg/g} \tag{2}$$

where, q_e is the equilibrium amount of dye adsorbed onto the adsorbents (mg g^{-1}), C_i the initial concentration of dye in the dye effluent (mg L^{-1}), C_e is the equilibrium concentration of the dye in solution (mg L^{-1}), V is the volume of the solution (L) and W is the weight of the adsorbent (g) q_e is average value of three experiments.

Column Mode. The unfixed dye in the dyebath was recovered using a glass column[24] filled with 10 g of powdered and sieved semi-IPN 21 without voids. Then, 100 mL of appropriated diluted RB 4 dye solution (1, 2, 3, 4, and 5 × 10^3 mg L^{-1}) was added to the column at a constant flow rate (2 mL min^{-1}) at 30°C. The effluent solution was collected at various time intervals after 30 min retention time within the column and the concentration of dye in solution was estimated spectrophotometrically at 573 nm. Similarly the adsorption capacity of semi-IPN 21 was tested for some commercial reactive dyes namely remazol black 13, reactive black 5, reactive red 189, reactive red 228 and reactive blue 19 under similar experimental conditions in column mode. An average of triplicate was used for the dye concentration. The equilibrium adsorption of RB 4 was calculated (Table I) using the mass balance eq. (2)

Adsorption Isotherm Modeling

The experimental equilibrium adsorption data for RB 4 onto semi-IPN 21 were fitted to four isotherms namely Langmuir, Freundlich, Temkin and Sips models to describe the interactive behavior between solutes and adsorbents.[25–28] These equilibrium data are essential for the practical design and operation of adsorption systems. In the present investigation the interactive behavior of dye-adsorbent was analyzed by fitting in Langmuir, Freundlich, Temkin and Sips models isotherm models as per eqs. (3)–(6) respectively.

$$\frac{1}{q_e} = \frac{1}{q_m} + \frac{1}{q_m K_L C_e} \tag{3}$$

$$\log q_e = \log K_F + N \log C_e \tag{4}$$

$$q_e = \frac{RT}{b_T} \ln a_T C_e \tag{5}$$

$$N \ln C_e = -\left(\frac{q_m}{q_e}\right) + \ln a_S \tag{6}$$

where q_m is the equilibrium monolayer adsorption capacity (mg g^{-1}), K_L is the Langmuir constant (L mg^{-1}) related to the adsorption energy which is a measure of the affinity between the adsorbent and adsorbate, K_F is Freundlich constant, which predicts the quantity of dye adsorbed (mg g^{-1}) per gram of polymer under equilibrium, N is a measure of the nature and strength of the adsorption process, b_T is the Temkin constant related to the heat of adsorption (kJ mol^{-1}), a_T is the equilibrium binding constant corresponding to the maximum binding energy (L mg^{-1}) and a_S is Sips constant related to energy of adsorption. The terms C_e and q_e have been defined earlier.

These isotherm models describe the equilibrium adsorption behavior of the dye on semi-IPN.

Adsorption Kinetics

The adsorption processes such as mass transfer and chemical reactions were tested with several kinetic models and reported elsewhere.[27–29] In the present investigation, the adsorption kinetics of RB 4 was tested using pseudo-first and second order kinetic models based on the eqs. (7) and (8) respectively.

$$\log (q_e - q_t) = \log q_e - \left(\frac{k_1}{2.303}\right) t \tag{7}$$

where q_e and q_t (both in mg g^{-1}) are amounts of RB 4 adsorbed at equilibrium and at time "t" respectively.

$$\frac{dq_t}{d_t} = k_2 (q_e - q_t)^2 \tag{8}$$

where k_1 (min^{-1}) and k_2 (g mg^{-1} min^{-1}) are the rate constants of adsorption for pseudo-first and second order kinetic models, respectively.

Thermodynamics of Dye Adsorption

The thermodynamic parameters are the actual indicators and are necessary to evaluate the practical applicability of an adsorbent. In the RB 4/semi-IPN system, the changes in the thermodynamic parameters namely, Gibbs free energy (ΔG°), enthalpy (ΔH°) and entropy (ΔS°) were determined[30] using eq. (9) and the spontaneity of the adsorption process was predicted using these parameters.

$$\ln K_d = \frac{\Delta S^\circ}{R} - \frac{\Delta H^\circ}{RT} \tag{9}$$

where K_d is the distribution coefficient of the adsorbate, ($K_d = C_e/q_e$), R is the universal gas constant (8.314 J K^{-1} mol^{-1}), T is the absolute temperature (K). The plot of $\ln K_d$ as a function of $1/T$ yields a straight line. From its slope and intercept, the average values of ΔH° and ΔS° were obtained respectively for the temperature range 303–323 K.

RESULT AND DISCUSSION

Mechanism of Semi-IPN Synthesis

The mechanism for the formation of semi-IPN is presented in Scheme 1. APS was used as a photo initiating agent for the

Table II. FT-IR Spectral Data for Typical Semi-IPN Samples and SAP

Types of bond stretching and their frequency range (cm^{-1})	Observed typical absorption frequencies of semi-IPN, SAP and NaAlg (cm^{-1})									
	semi-IPN 1	semi-IPN 4	semi-IPN 7	semi-IPN 14	semi-IPN 17	semi-IPN 20	semi-IPN 21	semi-IPN 24	semi-IPN 25	NaAlg	SAP
Aliphatic —CH_2 stretching (2936–2853)	2938	2935	2935	2932	2926	2935	2935	2933	2923	2925	2928
>C=O stretching in —C(=O)O— (1610–1550)	1615	1627	1623	1622	1613	1623	1610	1624	1617	1612	1618
Ester >C=O stretching (1750–1735)	1727	1727	1725	1730	1717	1722	1731	1728	1732	-	1730
>C—O stretching (1300–1100)	1118	1114	1109	1104	1106	1109	1106	1119	1120	1101	1163
Hydroxyl Free —OH stretching (3650–3590) (NaAlg)	3519	3525	3510	3515	3514	3514	3515	3510	3590	3502	-
—COOH >C=O bending (~1420)	1438	1433	-	1426	1431	1428	1425	1431	1451	-	1402
—COO^- group	1031	1032	1040	1024	1036	1036	1025	1034	1025	1029	-
Na-O (sodium alginate)	816	810	821	811	812	814	819	811	814	813	-
Amide >NH stretching (3500–3400)	3449	3445	3441	3443	3452	3456	3454	3453	3455	-	3456

crosslinking of partially neutralized poly (AA). Upon irradiation (254 nm) APS cleaves to yield two $SO_4^{\cdot -}$ radical anions. These radical anions generate reactive carbon-centered radicals. In the absence of radical scavengers, the carbon centered radicals combine to form non radical products.[31,32] But in the presence of oxygen during irradiation oxygen insertion reaction may also occur between the methine carbon and hydrogen (—C —H) leading to the formation of hydroperoxide (—C —O —O —H) weak links. As this link is photolabile which may result in the formation of oxygen centered radicals —C-O$^{\bullet}$ and H—O$^{\bullet}$ during photolysis[31,32] these may also induce crosslinking (Scheme 1).

FT-IR Analysis

Typical FT-IR spectra of semi-IPN, NaAlg and SAP were shown in Figure 1(b). The assignments of the absorption peaks for these IR spectra were given in Table II. Analysis of this data indicated the presence of crosslinker, monomeric unit and NaAlg moieties in the photo synthesized semi-IPN.[32–35] For example the absorption peaks around 1730 and 1620 cm^{-1} attributed to the >C═O stretching of ester group[20] (TMPTA) and carboxylate anion[20] (KA) respectively were present in both semi-IPN and SAP. The peaks at 1655–1660 cm^{-1} in all semi-IPN and SAP indicated the presence of NIPAAm moiety. The IR spectra also showed a broad peak at 3502 cm^{-1} (—OH), a peak at 1612 cm^{-1} is endorsed to —COO^-, and a peak at 1029 cm^{-1} corresponding to C—O group, which are characteristics peak of polysaccharide (NaAlg). The characteristic peak of sodium alginate appeared at 810–816 cm^{-1} (—Na—O) in all semi-IPN and NaAlg. Representative IR spectrums of virgin and recovered RB 4 are given in Figure1(c). The broad peaks at 3450 and 3455 cm^{-1} are attributed to the amino groups of virgin and recovered RB 4 respectively. Peaks at 1720, 1718 and 1639, 1636 cm^{-1} indicated the presence of exocyclic >C═O and endo cyclic >C═N groups in both the dyes. The characteristic peaks at 1139, 1146 and 679, 671 cm^{-1} correspond to >C—N and >C—Cl groups of these dyes and it corroborated the original chemical nature of the recovered RB 4.

Thermogravimetric (TG) Analysis

TG thermograms for representative semi-IPN 21, semi-IPN 25 and SAP are presented in Figure 3(a) showed multistep degradations. The initial weight loss up to 100°C was attributed to the residual volatile matters such as moisture present in the semi-IPN and SAP. The initial onset degradation temperature of semi-IPN around 210°C with considerable decomposition was ascribed to a complex process including dehydration of the saccharide rings, de-polymerization with the formation of water, CO_2 and methane.[33,36] The degradation step around 340°C is more likely due to the degradation initiated via the olefinic bonds, decarboxylation of carboxylate anion, scission of crosslinks,[20] and so forth, in both SAP and semi-IPN. The major degradation of semi-IPN 25 around 550°C corresponding to a weight loss of 50% is likely attributed to the degradation of NaAlg moiety. For the same feed composition, the higher degradation temperature corresponds to 20% weight loss at 680°C in semi-IPN 21 may be due to degradation of crosslinks which was formed by photo generated radicals.[34] Comparison of DTG curves revealed that the thermal stability of the semi-IPN 21 is

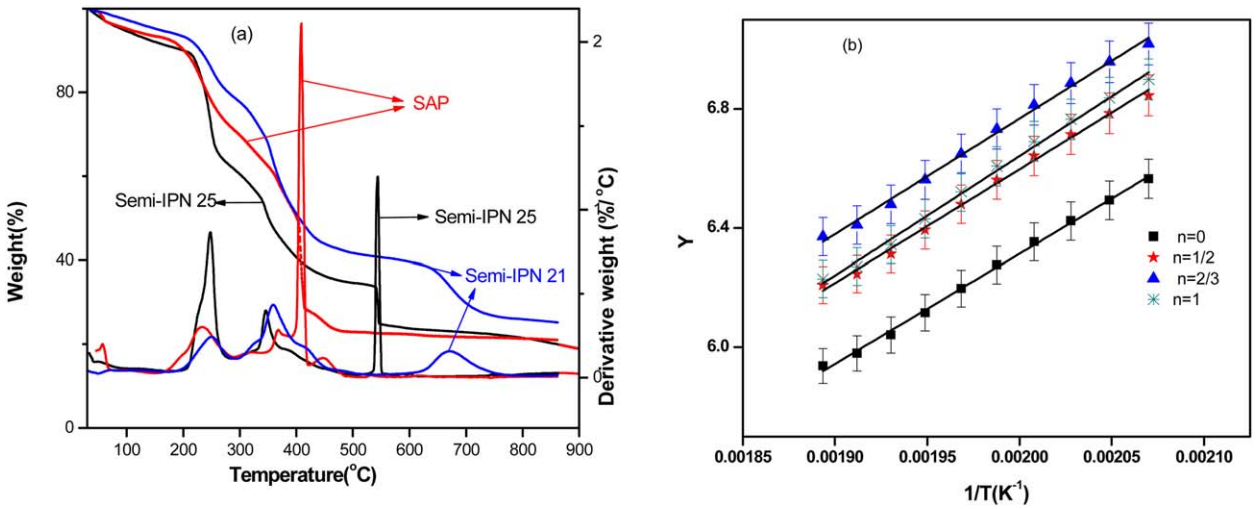

Figure 3. TG/DTG traces of (a) semi-IPN 21, semi-IPN 25, SAP and Arrhenius plots (b) from TG data for thermal degradation of semi-IPN 21. [Color figure can be viewed in the online issue, which is available at wileyonlinelibrary.com.]

greater than that of semi-IPN 25 and SAP. The higher thermal stability of semi-IPN 21 over semi-IPN 25 is due to higher APS concentration leads to high radial generation and crosslinks. This was also supported by the higher AE (Table III) for semi-IPN 21 over semi-IPN 25 and SAP. The TG analysis indicated that the thermal stability of semi-IPN 21 in air is good enough to withstand different adverse environmental conditions for continuous and prolonged applications.

Thermo Kinetic data

The kinetic data such as order and AE for thermal degradation of semi-IPN 21, semi-IPN 25 and SAP were determined using the weight loss data from single TG trace through the linear plot of Freeman and Carroll[20] eq. (10) for different values of "n".

$$Y=\log_{10}\frac{AR}{\alpha E}\left[1-\frac{2RT}{E}\right]-\frac{E}{2.3RT} \qquad (10)$$

where $Y=\log_{10}\left(\frac{1-(1-\alpha)^{1-n}}{T^2(1-n)}\right)$, α: degree of degradation, n: order, E: activation energy

The linear plots are obtained by plotting

1. Y versus $\frac{1}{T}$ for $n = 0, \frac{1}{2}$ and $\frac{2}{3}$, except $n = 1$
2. Y versus $\frac{1}{T}$ for $n = 1$,

Thermo kinetic parameters were determined from the slope and intercept of the best linear fit of Y versus $1/T$ [Figure 3(b)] for the above different values of "n" for semi-IPN 21, semi-IPN 25 and SAP. The kinetic order for the best linear fit seemed to be zero for these samples and the corresponding AEs were given in Table III.

Water Uptake and Dye Adsorption

Figure 4(a) showed dye and water uptake profiles of semi-IPN 21 with respect to time. The maximum equilibrium water uptakes by semi-IPN 21 and SAP were 993 and 1130 g g^{-1} respectively at 30°C. The dye adsorption capacities of semi-IPN 21 in column and batch mode were 624 and 597 mg g^{-1} respectively at 30°C, but SAP had adsorbed only 387 mg g^{-1} under ambient conditions. The adsorption capacity of semi-IPN 21 in column mode for remazol black 13 (reactive dye), reactive black 5, reactive red 189, reactive red 228 and reactive blue 19 dyes were given in Table IV. However, the adsorption capacities of the reported[37–41] adsorbent materials for these dyes were 130, 198, 180, 420, and 324 mg g^{-1}, respectively. The comparison of adsorption capacity of semi-IPN 21 with reported[37–41] material revealed that the dye adsorption capacity of semi-IPN 21 was significantly good enough for reactive dye recycling. Analysis of adsorption profiles revealed the water and dye uptake rates were greater than the corresponding release rates. The decrease in the release rates of water and dye may be due to the enhanced physico-chemical crosslinking through H-bonding with dye molecule.[20] However, in the absence of salts [Figure 4(b)] the adsorption capacity of semi-IPN 21 was around 898 mg g^{-1} (in the absence of co-ions). But at higher salt loading

Table III. Thermo Kinetic Parameters from TG Data for Semi-IPN 21, Semi-IPN 25 and SAP

Sample code	Tested kinetic order (n)	AE (kJ $mole^{-1}$)[a]	Kinetic order for the best fit
Semi-IPN 21	0	68.68	Zero
	1/2	71.65	
	2/3	72. 71	
	1	74.76	
Semi-IPN 25	0	52.38	Zero
	1/2	54.71	
	2/3	58.45	
	1	60.42	
SAP	0	31.45	Zero
	1/2	48.83	
	2/3	51.36	
	1	53.67	

[a] AE for the initial thermal degradation step (up to 220°C for semi-IPN and 200°C for SAP).

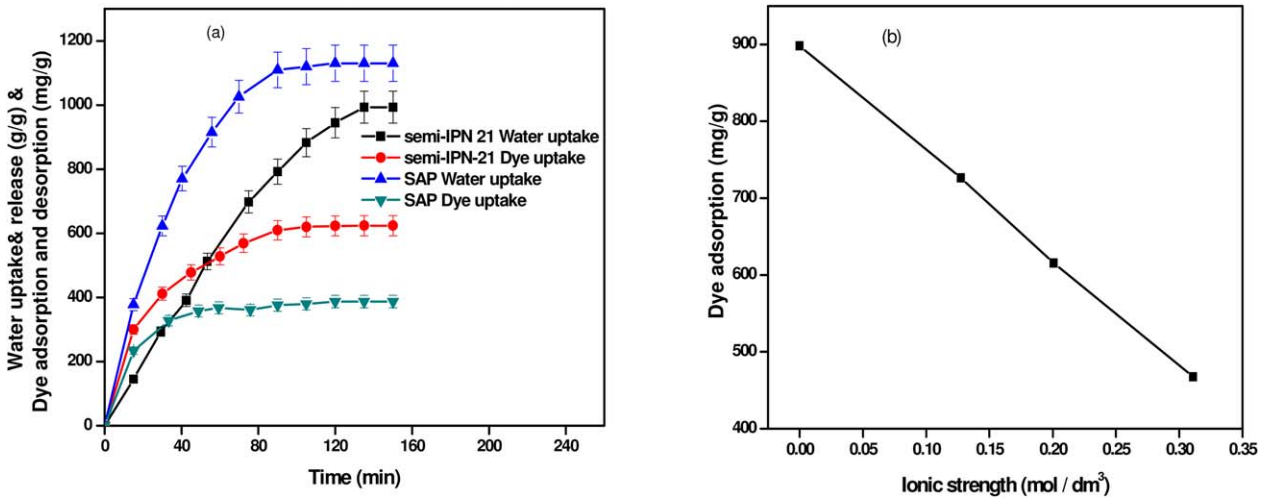

Figure 4. Water and RB 4 uptake profiles for semi-IPN 21 and SAP (a) effect of ionic strength on dye adsorption of semi-IPN 21 (b). [Color figure can be viewed in the online issue, which is available at wileyonlinelibrary.com.]

(Ionic strength = >0.2062 mol dm^{-3}) in the effluent the adsorption capacity decreased to 455 mg g^{-1}. Therefore the adsorption rate may be altered in the presence of co ions in the effluent.

SEM

The surface morphological features of freeze dried semi-IPN 21, SAP, RB 4 adsorbed semi-IPN 21 and dried semi-IPN 21 were analyzed by SEM and the representative SEM micrographs are shown in Figure 5. Analysis of these SEM images revealed the formation of pores during freeze drying [Figure 5(a,b,d)] and porous network structure in irradiated samples. The porous morphology is more likely due to water evaporation in all swollen hydrogel. The shapes of the pores are irregular and interconnected. The massive distribution of pores in the freeze dried samples indicated water uptake throughout the material and the presence of void volume. The unequal pore sizes may imply that the crosslinking may not be uniform throughout the material. The porous structure appeared to be more compact in SAP possibly due to intermolecular crosslinking. These porous may be the areas, where the water permeation occurs and interaction sites are available to form secondary bonds with dyes, metal ions, drugs, and so forth.[42–45] Analysis of Figure 5(c,d) also confirms the absence of pores and void volume in dried and powdered semi-IPN 21, and adsorption of RB 4 on semi-IPN 21. Hence, the porous structure appeared to be the predominant cause for the high swellability and dye adsorption. The analysis of SEM micrographs of semi-IPN 21 revealed NaAlg was dispersed in the continuous phase of TMPTA crosslinked poly (AA/KA-NIPAAm) hydrogel.

Mechanical Properties

Under modest compression the water swollen SAPs are fragments into pieces due to its insubstantiality. But the photo crosslinked semi-IPN was able to withstand cycles of compression and regains its original shape on relieving the compression as shown in Figure 2. Moreover, the semi-IPN 21 can able to hold water and water soluble material through adsorption even under compression unlike SAP. This demonstrated that semi-IPN having significantly improved mechanical properties in terms of elongation and modulus. Figure 2(e) shows typical compressive stress–strain curve of semi-IPN 21 and SAP. The representative semi-IPN 21 gel showed a compressive elastic modulus 788 MPa, which is very much greater than that of SAP (55 MPa). The ultimate stress and the strain at the breaking (failure) point of semi-IPN 21 and SAP were 39.4 (at % elongation 388) and 2.98 MPa (at % elongation 2.75) respectively. Hence the adsorbent may be persistently used for textile effluent treatment process.

Adsorption Isotherms

The interactive behaviors of adsorbate with adsorbent were described by equilibrium adsorption isotherms as shown in Figure 6 and the isotherm data for RB 4 on semi-IPN 21 was fitted to Langmuir, Freundlich, Temkin and Sips isotherms. The best fit [correlation coefficient (R^2, 0.991] was observed with Langmuir model [Figure 6(a)] indicating monolayer dye adsorption.[27] This was also supported by the nearly identical values for the experimentally determined equilibrium dye adsorption and theoretically calculated equilibrium RB 4 adsorption for Langmuir isotherm model on semi-IPN 21. Langmuir isotherm parameters q_m and K_L calculated from the slope and intercept of the plot [Figure 6(a)] were 641 mg g^{-1} and 0.102 L mg^{-1}, respectively for column mode adsorption of RB 4 on semi-IPN 21. Langmuir isotherm is an outstanding isotherm model and is

Table IV. Adsorption Capacity of Semi-IPN 21 for Some Reactive Dyes

Sample code	Name of the reactive dye	Adsorption capacity (column mode, mg g^{-1})
semi-IPN 21	Remazol black 13 (reactive) dye	598
	Reactive black 5	603
	Reactive red 189	644
	Reactive red 228	587
	Reactive blue 19	431

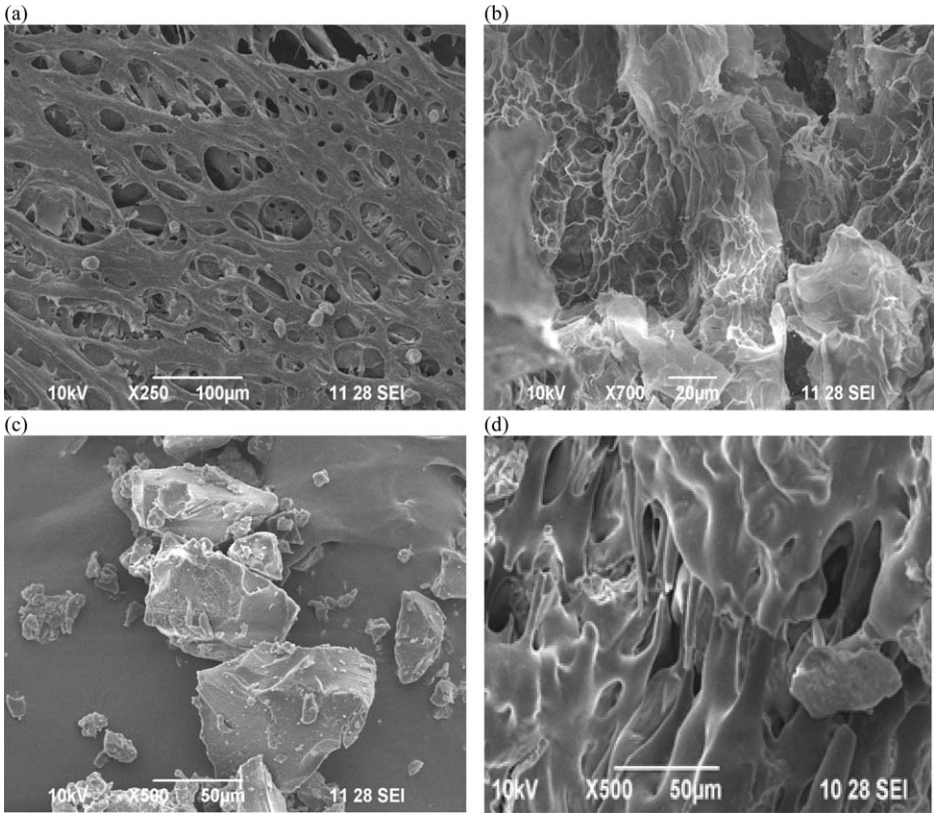

Figure 5. SEM micrographs of freeze dried, lyophilized semi-IPN 21(a), SAP(b), RB 4 adsorbed semi-IPN 21(d) and powdered semi-IPN 21(c).

being frequently used to quantify the performance of different adsorbents.[27,28]

Adsorption Kinetics

The rate of adsorption an important parameter is essential for column design and process optimization for successful commercial application of an adsorbent such as heavy metal and textile dye removal from effluent. Comparing the adsorption capacities (mg g^{-1}) of semi-IPN 21 and SAP for RB 4 measured as a function of time [Figure 4(a)] revealed rapid dye adsorption during the initial 60 min of contact time, which subsequently slowed down over a longer period of time until the equilibrium was attained. During the initial 60 min contact time, 80% of equilibrium adsorption for semi-IPN 21 was accounted. The rapid dye adsorption[28,29] is most probably due to the abundant availability of active sites on the adsorbent, whereas with the gradual occupancy of these sites, adsorption became less efficient after 60 min of contact time. The degree of dye adsorption was tested with the pseudo-first order and pseudo-second order kinetics models by comparing the R^2 values using the plot "$\log(q_e - q_t)$ versus t" and t/q_t versus t, respectively (Figure 7). This implied that the dye adsorption followed[28,29] pseudo second-order kinetics. The rate constants of adsorption determined from the slopes of profiles in Figure 7(a,b) were decreased with temperature, indicating enhanced temperature does not favor the adsorption of RB 4. The extent of dye adsorption, and the amount of dye adsorbed per unit mass of the adsorbents (q_e) decreased appreciably with temperature which may be attributed to the competing desorption process as well as supply of excess energy that promote desorption at enhanced temperatures.

Thermodynamics of Dye Adsorption

In adsorption studies, changes in both energy and entropy should be considered to determine spontaneity of the reaction, and the ΔG°, ΔH° and ΔS° values for dye adsorption were measured as per the eq. (9). The negative values of ΔG° namely, -19.73, -20.47 and -21.20 kJ mol^{-1} for the temperature 303, 313 and 323 K, respectively indicated that the RB 4 adsorption on semi-IPN 21 was spontaneous and confirmed affinity of sorbent for the dyes. The average negative value of ΔH° (-12.04 kJ mol^{-1}) for the above temperatures indicated adsorption is exothermic which may be due to the weak interactions between the adsorbent and dye molecules. The positive value of entropy (4.19 kJ mol^{-1}) was attributed to the increased volume of the system (adsorbent and dye solution) through swelling which may enhance the mobility of the adsorbed dye molecule during the adsorption of RB 4 on semi-IPN 21. The above discussed observations indicated that the semi-IPN 21 is a good candidature material for recycling of dye[46,47] from the textile dye effluent.

Kinetics of Water and RB 4 Diffusion

The dye and water uptake kinetics of semi-IPN 21 can be more quantitatively understood by fitting the initial swelling data (up-to 60%) of semi-IPN 21 in power law[48] eq. (11)

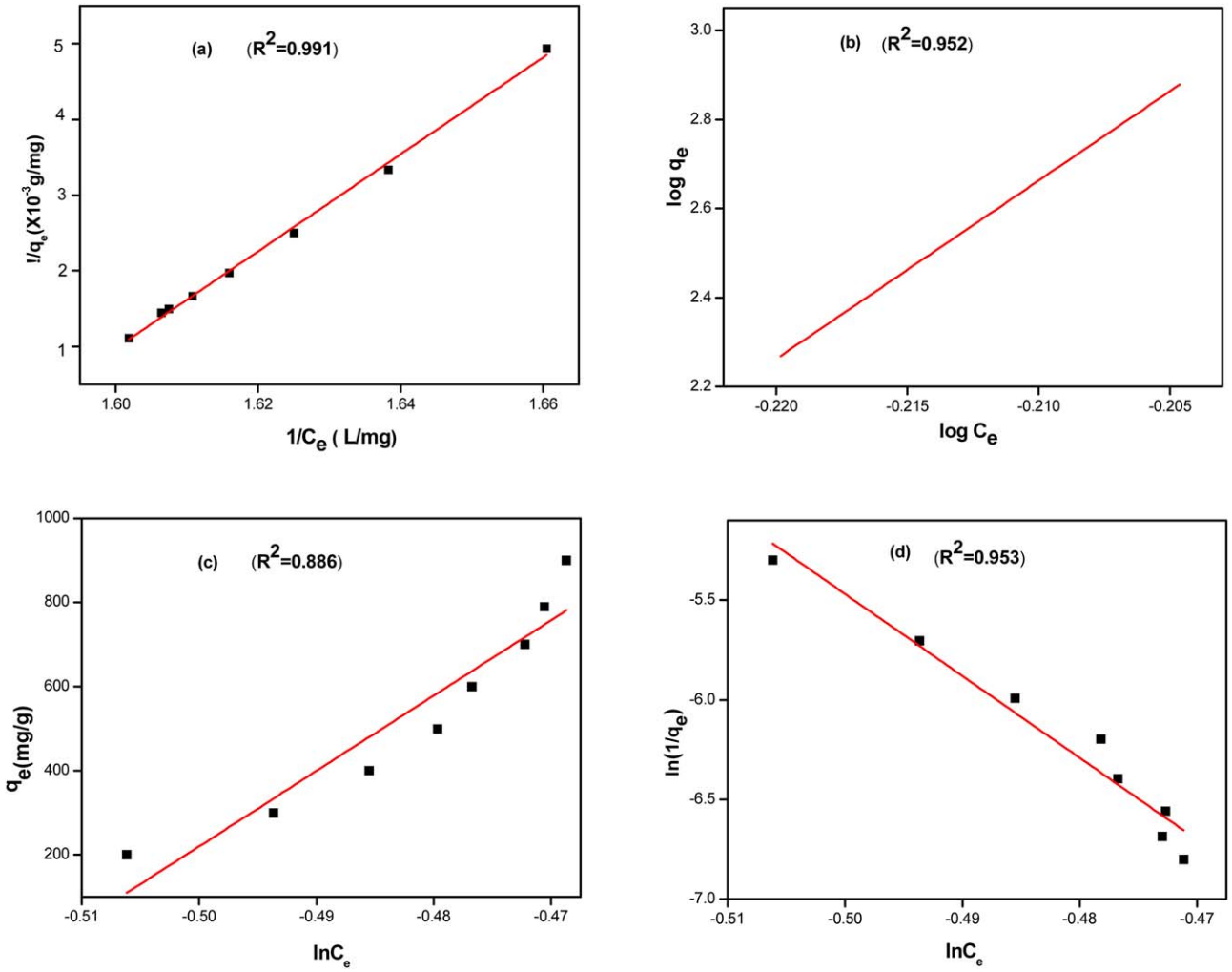

Figure 6. Langmuir (a), Freundlich (b), Temkin (c) and Sips (d) adsorption isotherms model for semi-IPN 21/RB 4 system. [Color figure can be viewed in the online issue, which is available at wileyonlinelibrary.com.]

$$\frac{M_t}{M_\infty} = kt^n \tag{11}$$

where M_t = amount of the water/or dye adsorbed by the swollen polymer at time t, M_∞ = amount of the water/or dye adsorbed under equilibrium condition, k = swelling constant related to the structure of network and n = diffusion exponent, the values of n and k were calculated from the slopes and intercepts of the plot of $\log(M_t/M_\infty)$ against $\log(t)$, at different temperature, respectively. . In case of adsorption/or release from swellable matrices, if n = 0.5 then transport is Fickian. For n = 1, the zero order adsorption is operative, whereas for $n > 1$, transport is super Case-II. In the present investigation the values of 'n' were found to be in the range of 0.35–0.42 and 0.66–0.69 with dye solution and pure water respectively. These values indicate that the diffusion of dye in the swollen polymer and diffusion of water in water swollen polymer both followed non-Fickian[48] mechanism. The non-Fickian nature of the dye and water molecule transport during swelling of matrix may be attributed to the segmental mobility of the semi-IPN.

Reusability of Dye and Adsorbent

The reusability and reliability of the adsorbent was tested during the repeated adsorption–desorption cycle of it usage. It was observed that the adsorption capacity of semi-IPN 21 for RB 4 was 624 mg g^{-1}. The adsorption capacity remains nearly constant after five adsorption–desorption cycle demonstrating that semi-IPN 21 may be repeatedly used for the removal of reactive dye from textile dye effluent in the column mode in commercial effluent treatment plants due to the improved mechanical properties over SAP. The nearly identical molar extinction coefficients values at 573 nm (λ_{max}) for the virgin (865,550 L mol^{-1} cm^{-1}) and recovered RB 4 (865,932 L mol^{-1} cm^{-1}) indicated that the dye remain chemically intact after repeated adsorption–desorption cycle. The solid state visible absorption spectra (Figure 8) for the cloth dyed using virgin and recovered dye were nearly identical corroborating the chemical stability of the dye during dye recovery processes in column mode. Besides, IR spectrum of virgin RB 4 and recovered RB 4 were identical even after five adsorption–desorption cycles demonstrating that the dye remained stable structurally and hence the recovered RB 4

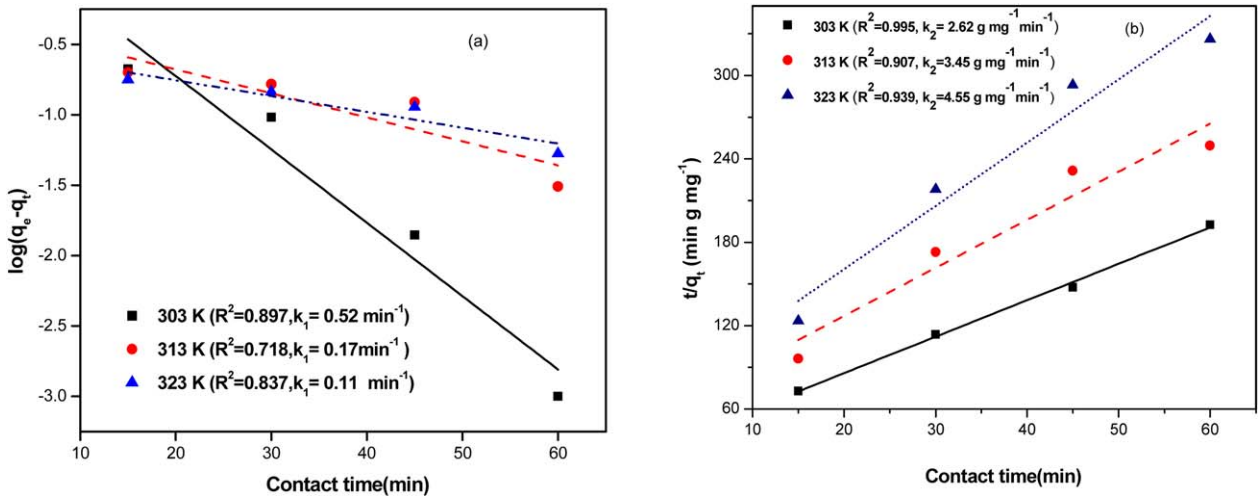

Figure 7. Pseudo first (a) and second (b) order adsorption kinetics plots at different temperatures, for RB 4 and semi-IPN 21 systems. [Color figure can be viewed in the online issue, which is available at wileyonlinelibrary.com.]

may be reused for dying fabrics. The constant color fastness properties of the dyed fabric with RB 4 and recovered RB 4 also supported that the original chemical nature of recovered dye remained same, and the dyed fabrics showed good color fastness under sunlight and also in soap solution.

Factors Affecting Dye adsorption

Feed Composition. ***AA salt and AA ratio(S/A), NIPAAm, TMPTA and NaAlg.*** The nature and percentage of monomers incorporated in semi-IPN may greatly influence its quantum of water dye and uptakes. The profiles for water (g g^{-1}) and dye (mg g^{-1}) absorption in terms of uptake versus time for typical semi-IPN with various values of *S*/*A* are given in given in Figure 9(a). The maximum dye uptake was obtained for *S*/*A* = 0.5723. When, *S*/*A* values > 0.0573, a significant reduction in water as well as dye uptakes were noticed. This was mainly attributed to the more hydrogen bonding at lower values of *S*/*A*, and osmatic pressure effect.[20] In addition, at *S*/*A* values >0.0572, physical crosslinking via H-bonding may be reduced. The water and dye uptake profiles with respect to time for typical semi-IPN prepared using different concentrations of NIPAAm are displayed in Figure 9(b). Increased concentration of NIPAAm in the feed displayed an increased water uptake for low *S*/*A* values in the feed. The swellability of the synthesized semi-IPN prepared using low concentration of NIPAAm showed a decrease in ES due to the weakening of the hydrogen bonding between the carboxylic acid groups and water, and synergistic effect of the different hydrophilic groups.[20] ES was increased till the concentration of NIPAAm reached 0.0625 *M*, and decreased with increased concentration of NIPAAm (beyond 0.0625 *M*).

Crosslinker concentration, a key factor which affecting the water and dye uptakes of semi-IPN, and the uptake behavior was directly proportional to lower crosslinker concentration and inversely proportional to it at higher crosslinker concentrations.[20] Since the water absorbency can be altered with a small change in crosslinker concentration in the feed composition. The hydrogel network with different crosslinker levels were prepared and evaluated by their water absorption and release characteristics. The influence of crosslinker level on water uptake profile is shown Figure 9(c). For the crosslinker concentration 0.005 *M*, water and dye uptakes were increased to the maximum extent of 1130 g g^{-1} and 624 mg g^{-1}, respectively.

With the increased crosslinker concentration beyond 0.005 *M* (Table I) for the constant concentrations of other ingredients both water and dye uptake were decreased. The higher crosslinker concentration (>0.005 *M*) may decreased the space among the grids of the three-dimensional network of hydrogel leading to decrease in uptake behavior of semi-IPN. In addition to that the physical crosslinking may also significantly influence both water and dye uptakes.[20] For the various concentrations of the crosslinker below 0.005 *M* with constant concentrations of other ingredients also leads to decreased water and dye uptakes, and this may be due to poor physico chemical crosslinking. The amount of NaAlg in the feed also altered the water and dye uptake behavior of semi-IPN 21 as shown in Figure 9(d). The

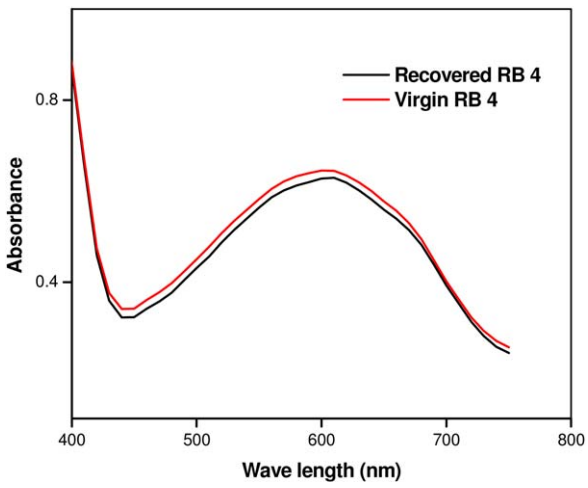

Figure 8. Solid state visible absorption spectra of virgin and recovered RB 4 dyed specimen. [Color figure can be viewed in the online issue, which is available at wileyonlinelibrary.com.]

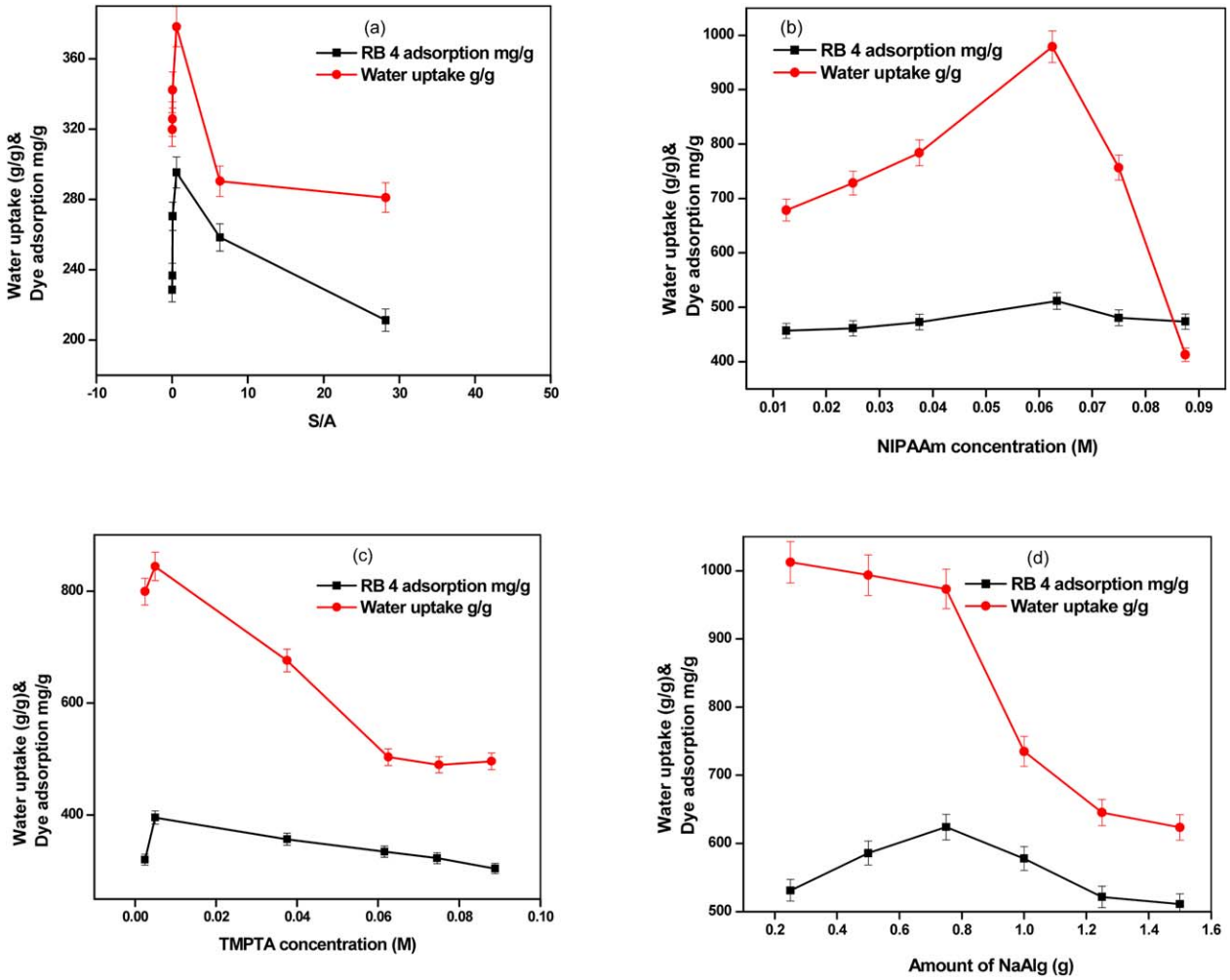

Figure 9. Influence of *S/A* (a), NIPAAm concentration (b), TMPTA concentration(c) and NaAlg content (d) on water uptake (g g^{-1}) and RB 4 dye adsorption (mg g^{-1}). [Color figure can be viewed in the online issue, which is available at wileyonlinelibrary.com.]

increased dye uptake was observed till the weight of NaAlg reached to 0.75 g (constant concentrations of other ingredients). Further increase (beyond 0.75 g) of NaAlg content the dye and water uptake decreased significantly. This could be attributed to the poor physico-chemical crosslinking between monomer and crosslinker residue and electrostatic repulsion between carboxylate anions as well.

APS Concentration. The equilibrium dye and water uptake capacity of semi-IPN 21 was investigated as a function of different initiator concentration as shown in Figure 10(a). The uptake behaviors of the adsorbent had increased till it reaches the 0.009 *M* concentration of APS and the obtained maximum water and dye uptakes were 993 g g^{-1} and 624 mg g^{-1}, respectively. The reduction of uptake beyond 0.009 *M* APS may be attributed to an increase of chain termination reactions via bimolecular collision[49] (this reason is referred to as self-crosslinking) and radical generation in NaAlg may leads to extensive cross linking. In the absence of APS with the minimum dose of irradiation time ($\leq$ 6 h) the water and dye uptake was reduced drastically. This may be due to less number of radicals generation in the monomeric unit as a function of decreased APS concentration. Hence, the network cannot be formed efficiently with this few numbers of radicals during free-radical polymerization reaction,[50] which may decreased the water and dye uptakes to some extent.

Irradiation Time. Duration of irradiation has also altered the dye adsorption behavior of semi-IPN for a given composition of semi-IPN 21 as shown in Figure 10(b). The semi-IPN 21 (6 h irradiated) had absorbed 993 g g^{-1} of water under ambient conditions. However it had adsorbed 624 and 781 mg g^{-1} of dye in effluent and distilled water, respectively. For irradiation time beyond 6 h, the water uptake and dye adsorption were reduced drastically and this may be attributed to extensive crosslinking between vinylic monomers and crosslinker molecules. The identical viscosity values and flow time (Ostwald viscometer) of virgin and 6 h irradiated NaAlg also supports the lack of proton abstraction and radical generation on NaAlg.

pH Values. The pH value of dye effluent is one of the major factors that affecting the dye adsorption behavior of an adsorbent, and it was investigated over a pH range of 2–10 are given in Figure 10(c). The functional groups on the surface of an adsorbent may be altered by the variation in pH of dye effluent

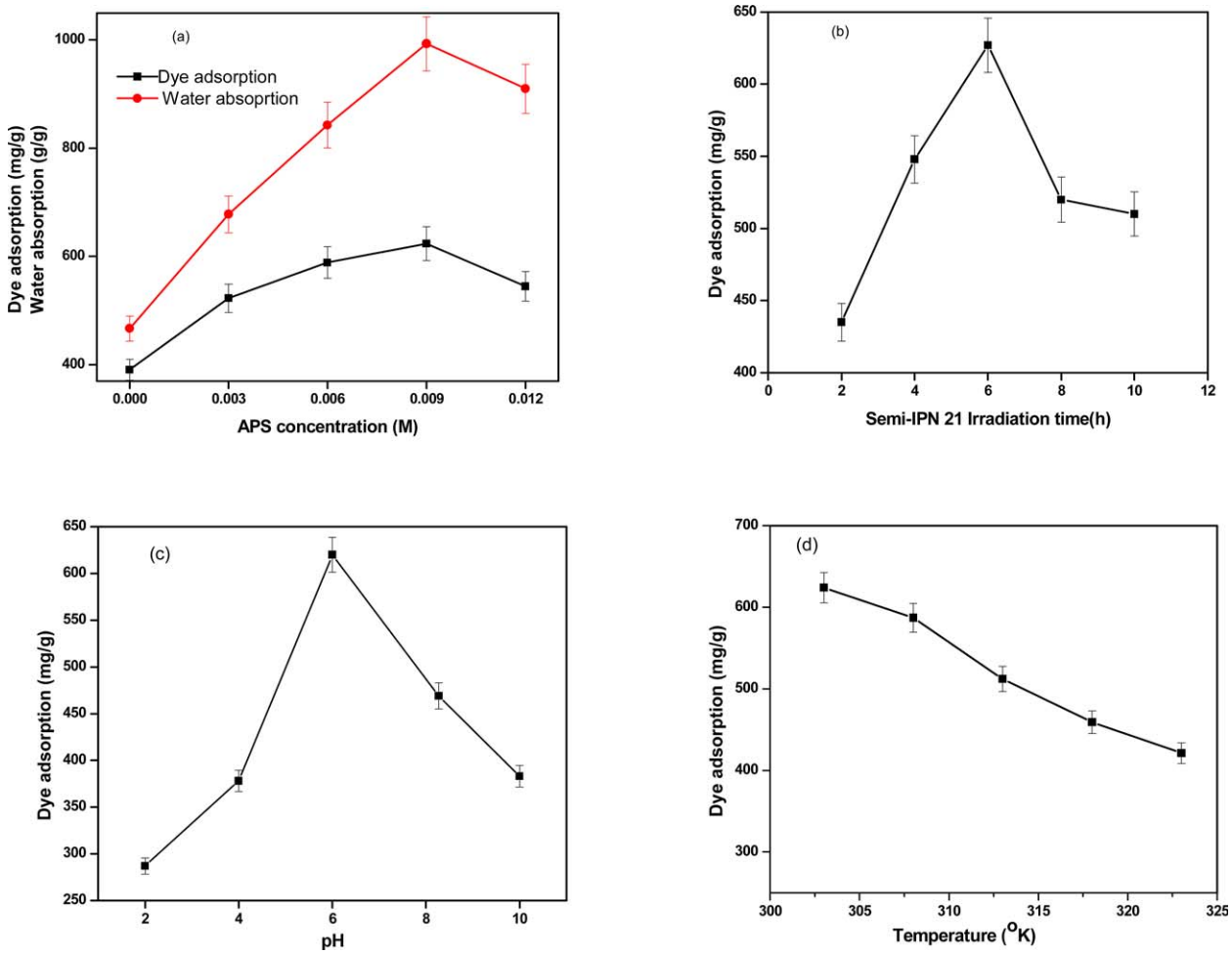

Figure 10. Effect of APS concentration (a), irradiation time (b), pH (c), and temperature (d) on dye adsorption. [Color figure can be viewed in the online issue, which is available at wileyonlinelibrary.com.]

taken for treatment process. It was obvious that the adsorption capacity increased with increasing pH of dye effluent, and significant enhancement was observed till it reached a pH of 6 and further increase of pH beyond 8 had reduced the dye adsorption. In acidic pH most of the carboxyl groups on the surface of the adsorbent exist in the form of —COOH, which lead to a competition between hydrogen ion and RB 4 to seek the active site on the adsorbent. This may result in the reduction of dye adsorption. At higher pH (beyond 8) the electrostatic repulsive force between adsorbent and adsorbate may diminish[51,52] the dye adsorption on semi-IPN 21.

Temperature. The effect of temperature on the uptake behavior of semi-IPN 21 was investigated for the temperatures range 303–323 K. The temperature profiles for water absorption of semi-IPN 21 are given in Figure 10(d). A maximum of 624 mg g^{-1} of dye adsorption was absorbed at 303 K. When the temperature was increased beyond 303 K the decreased dye uptake was observed. This could be attributed to the temperature dependence association/dissociation of the hydrogen bonding by the hydrophilic groups of the copolymer[20] and chemically crosslinked NIPAAm may also showed phase transitional behavior with respect to changes in external temperature.[53]

CONCLUSIONS

Semi-IPNs with different compositions were synthesized photo chemically using APS as photo initiator at 254 nm. Studies on TG and mechanical properties of representative semi-IPNs revealed that they are thermally and mechanically stable under usual environmental conditions. SEM micrographs of swelled, freeze dried and lyophilized semi-IPN 21 implied that NaAlg was dispersed in continuous phase of TMPTA crosslinked poly (AA/KA-NIPAAm). In every adsorption–desorption cycle nearly constant amount of (624 mg g^{-1}) dye was recovered for a frequency of five cycles. The originality of recovered RB 4 was confirmed by visible absorption spectra and constant color fastness properties of dyed fabrics. The equilibrium dye adsorption profiles at different dye concentrations implied predominantly Langmuir adsorption isotherm and the kinetic data of adsorption followed pseudo-second order model. The water and dye diffusion inside the semi-IPN matrix followed non-Fickian mechanism. The values of ΔG°, ΔH° and ΔS° for the RB 4 dye adsorption indicated that adsorption is a spontaneous and exothermic process for the chosen semi-IPN 21. This study demonstrated that semi-IPN 21 can serve as a potential adsorbent for the effective recycling of reactive dyes from the textile effluent in commercial textile effluent treatment plants.

ACKNOWLEDGMENTS

The authors thank the management of Bannari Amman Institute of Technology, Sathyamangalam for encouraging research work by extending the required facilities.

REFERENCES

1. Orthman, J.; Zhu, H. Y.; Lu, G.Q. *Sep. Purif. Technol.* **2003**, *31*, 53.
2. Nasr, M. F.; Abo El-Ola, S. M.; Ramadan, A.; Hashem, A. *Polym. Plast. Technol.* **2006**, *45*, 335.
3. Kadirvelu, K.; Brasquet, C.; Cloiree, P. *Langmuir* **2000**, *16*, 8404.
4. Rajeswari, S.; Namasivayam, C.; Kadirvelu, K. *Waste Manage.* **2001**, *21*, 105.
5. Tahir, S. S.; Rauf, N. *Chemosphere* **2006**, *63*, 1842.
6. Baskaralingam, P.; Pulikesi, M.; Ramamurthi, V. S.; Sivanesan, *J. Hazard. Mater.* **2006**, *136*, 989.
7. Dhodapkar, R.; Rao, N. N.; Pande, S. P.; Kaul, S. N. *Bioresour. Technol.* **2006**, *97*, 877.
8. Tsai, W. T.; Chang, C. Y.; Ing, C. H.; Chang, C. F. J. *J. Colloid Interface Sci.* **2004**, *275*, 72.
9. Li, S. *Bioresour. Technol.* **2010**, *101*, 2197.
10. Yamak, O.; Ayca Kalkan, N.; Aksoy, S.; Altinok, H.; Hasirci, N. *Process Biochem.* **2009**, *44*, 440.
11. Wang, J. J.; Liu, F. *Polym. Bull.* **2013**, *70*, 1415.
12. Wenceslau, A. C.; Santos, F. G. D.; Ramos, É. R. F.; Nakamura, C. V.; Rubira, A. F.; Muniz, E. C. *Mater. Sci. Eng. C* **2012**, *32*, 1259.
13. Saber-Samandari, S.; Elvan Yilmaz, M.G. *Polym. Bull.* **2012**, *68*, 1623.
14. Ecaterina Stela, D.; Diana Felicia, A. *Chem. Eng. J. 011*, *178*, 252.
15. Gong, J. P.; Katsuyama, Y.; Kurokawa, T.; Osada, Y. *Adv. Mater.* **2003**, *15*, 1155.
16. Nakajima, T.; Furukawa, H.; Tanaka, Y.; Kurokawa, T.; Osada, Y.; Gong, J. P. *Macromolecules* **2009**, *42*, 2184.
17. Marandi, G. B.; Sharifnia, N.; Hosseinzadeh, H. *J. Appl. Polym. Sci.* **2006**, *101*, 2927.
18. Zendehdel, M.; Barati, A.; Alikhani, H. *Polym. Bull.* **2011**, *67*, 343.
19. Kobašlija, M.; Tyler McQuade, D. *Biomacromolecules* **2006**, *7*, 2357.
20. Dhanapal, V.; Vijayakumar, V.; Subramanian, K. *J. Appl. Polym. Sci.* **2013**, *129*, 1350.
21. Nakayama, A.; Kakugo, A.; Gong, J. P.; Osada, Y.; Erata, M. T.; Kawano, S. *Adv. Funct. Mater.* **2004**, *14*, 1124.
22. Jeon, Y. S.; Lei, J.; Ji-Heung, K. *J. Ind. Eng. Chem.* **2008**, *14*, 726.
23. Riera-Torres, M.; Maria-Carmen, G. *Chem. Eng. J.* **2010**, *156*, 114.
24. Vijaya, Y.; Popuri, V. M.; Boddu, S. R.; Krishnaiah, A. *Carbohydr. Polym.* **2008**, *72*, 261.
25. Haque, M. A.; Kurokawa, T.; Gong, J. P. *Polymer* **2012**, *53*, 1805.
26. Langmuir, I. *J. Am. Chem. Soc.* **1918**, *40*, 1361.
27. Apopei, D. F.; Dinu, M. V.; Trochimczuk, A. W.; Stela Dragan, E. *Ind. Eng. Chem. Res.* **2012**, *51*, 10462.
28. Uma; Banerjee, S.; Sharma, Y. C. *J. Ind. Eng. Chem.* **2013**, *19*, 1099.
29. Acharya, J.; Sahu, J. N.; Sahoo, B. K.; Mohanty, C. R.; Meikap, B. C. *Chem. Eng. J.* **2009**, *150*, 25.
30. Bhattacharyya, K. G.; Gupta, S. S. *J. Colloid Interface Sci.* **2007**, *310*, 411.
31. Decker, C. *Eur. Polym. J.* **1984**, *20*, 149–155.
32. Jockusch, S.; Turro, N. J.; Mitsukami, Y.; Matsumoto, M.; Iwamura, T.; Lindner, T.; Flohr, A.; Massimo, G. *J. Appl. Polym. Sci.* **2009**, *111*, 2163.
33. Isıklan, N.; Kursun, F.; Inal, M. *Carbohydr. Polym.* **2010**, *79*, 665.
34. Solpan, D.; Torun, M.; Guven, O. *J. Appl. Polym. Sci.* **2008**, *108*, 3787.
35. Pawar, S. N.; Edgar, K. J. *Biomaterials* **2012**, *33*, 3279.
36. Wang, W.; Wang, A. *Carbohydr. Polym.* **2010**, *80*, 1028.
37. Tae-Young K.; Seung-Shik P.; Sung-Yong C. *J. Ind. Eng. Chem.* **2012**, *18*, 1458.
38. Chiou, M. S.; Li, H. Y. *Chemosphere* **2003**, *50*, 1095.
39. Wang, L.; Zhang, J.; Wang, A. *Desalination* **2011**, *266*, 33.
40. Wang, L.; Li, J. *Ind. Crop. Prod.* **2013**, *42*, 153.
41. Hasan, M.; Ahmad, A. L; Hameed, B. H. *Chem. Eng. J.* **2008**, *136*, 164.
42. Pourjavadi, A.; Barzegar, S. *Starch-Starke* **2009**, *61*, 161.
43. Selva, C.; Gurdag, G. *Polym. Adv. Technol.* **2008**, *19*, 1209.
44. Pourjavadi, A.; Jahromi, P. E.; Seidi, F.; Salimi, H. *Carbohydr. Polym.* **2010**, *79*, 933.
45. Attaa, A. M.; Adel Abdel-Rahmanb, A.-H.; El Aassyc, I. E.; Ahmedc, F. Y.; Hamzac, M. F. *J. Dispersion Sci. Technol.* **2011**, *32*, 84.
46. Olgun, A.; Atar, N. *J. Ind. Eng. Chem.* **2012**, *18*, 1751.
47. Coskun, R. *Polym. Bull.* **2011**, *67*, 125.
48. Ritger, P.; Peppas, N. *J. Controlled Release* **1987**, *5*, 37.
49. Pourjavadi, A.; Bardajee, G. R.; Soleyman, R. *Starch–Starke* **2008**, *60*, 467.
50. Li, A.; Wang, A. *Eur. Polm. J.* **2005**, *41*, 1630.
51. Zohra, B.; Aicha, K.; Fatima, S.; Nourredine, B.; Zoubir, D. *Chem. Eng. J.* **2008**, *136*, 295.
52. Liu, Y.; Zheng, Y. Wang, A. *Ionics* **2011**, *17*, 535.
53. Zhao, S. P.; Zhou, F.; Yan Li, L. *J. Polym. Res.* **2012**, *19*, 9944.